Biochimica et Biophysica Acta 1817 (2012) 269–275

Contents lists available at SciVerse ScienceDirect

Biochimica et Biophysica Acta

journal homepage: www.elsevier.com/locate/bbabio

Electrogenic events upon photolysis of CO from fully reduced cytochrome *c* oxidase

Marko Rintanen, Ilya Belevich *, Michael I. Verkhovsky [1]

Helsinki Bioenergetics Group, Institute of Biotechnology, University of Helsinki, PB 65 (Viikinkaari 1), 00014, Helsinki, Finland

ARTICLE INFO

Article history:
Received 5 August 2011
Received in revised form 7 November 2011
Accepted 9 November 2011
Available online 18 November 2011

Keywords:
Potential generation
Proton transfer
Potential electrometry
Molecular bioenergetics

ABSTRACT

CO photolysis from fully reduced *Paracoccus denitrificans* aa_3-type cytochrome *c* oxidase in the absence of O_2 was studied by time-resolved potential electrometry. Surprisingly, photo dissociation of the uncharged carbon monoxide results in generation of a small-amplitude electric potential with the same sign as the physiological charge separation during activity. The number of electrogenic events after CO photolysis depends on the state of the enzyme. CO photolysis following immediately after activation by an enzymatic turnover, showed a two-component potential development. A fast (~1.5 μs) phase was followed by slower potential generation with a time constant varying from 8 μs at pH 7 to 250 μs at pH 10. The amplitude of the fast phase was independent of the time of incubation after enzyme activation, whereas the slower phase vanished with a time constant of ~25 min. CO photolysis from enzyme that had not undergone a prior single turnover showed the fast phase, but the amplitude of the slow phase was reduced to 10–30%. The amplitude of the fast phase corresponds to charge movement of 0.83 Å perpendicular to the membrane dielectric, and is independent of the time after enzyme activation. Thus it can be used as an internal ruler for normalization of the electrogenic responses of C*c*O. The slow phase was absent in the K354M mutant with a blocked proton-conducting K channel. We propose that CO photolysis increases the pK of the K354 residue, which results in its partial protonation, and generation of electric potential.

1. Introduction

Cytochrome *c* oxidase (C*c*O) is the terminal enzyme of the electron transfer chain located in the inner membrane of mitochondria, and in the plasma membrane of many species of aerobic bacteria. There are two parallel mechanisms by which C*c*O catalysis is coupled to the generation of electrochemical proton gradient. Half of the energy conservation is the result of the vectorial nature of the oxygen reduction chemistry itself [1]: the enzyme uses four electrons delivered from cytochrome *c* at the positively charged outer side of the membrane (P side) while four protons are taken from the inner side (N side). As a result, the reduction of each molecule of oxygen to water is coupled to translocation of four electrical charges across the membrane. In addition, C*c*O uses the energy of this redox reaction to pump four additional charges (protons) per oxygen from the N- to the P side of the membrane [2]. The detailed molecular mechanism of the proton pump is still not known, and is subject to intense investigation [3–6].

It is well established that during the enzyme's catalytic cycle there is a large number of different electron and proton transfer events with a great variety of rates. Detailed understanding of the topology of all these charge translocations should provide significant help in understanding the molecular mechanism. Therefore, the method of time-resolved potential electrometry [7,8], which provides the ability for precise determination of relative charge displacements, is a powerful tool for investigating the C*c*O mechanism and for creating a "dielectric topography" map of the enzyme [9]. However, the amplitudes of the electrometric response give only a relative displacement without direct information about the exact number of moved charges. The amplitudes may be converted into a number of moved charges only when there is an internal molecular “ruler” to which the displacement can be normalized. For example, in photosynthetic reaction centers with well-known 3D structure [10], the ultra-fast charge separation between the chlorophyll special pair and the primary quinone corresponds to the movement of a single charge over an exactly established distance, and this phase of charge separation can be used for calibrating all other charge translocation events in the sample [11,12].

In this paper we make an attempt to find such an internal molecular “ruler” for the charge transfer reactions in C*c*O. We used the ability of potential electrometry to distinguish very small electrical changes in the enzyme to show that a 1.5 μs phase of potential generation upon CO photolysis from fully reduced C*c*O is proportional to the enzyme concentration and does not depend on experimental conditions (such as pH, enzyme activation, different single point mutations), and can thus be used as an internal calibration for other charge movement events in C*c*O, for example, the **R** (fully reduced) to $\mathbf{O_H}$ (oxidized) transition upon addition of molecular oxygen.

Abbreviations: C*c*O, type aa_3 cytochrome *c* oxidase; DM, *n*-dodecyl-β-D-maltoside; E_h, ambient redox potential; E_m, midpoint redox potential

* Corresponding author.
E-mail address: Ilya.Belevich@Helsinki.Fi (I. Belevich).

[1] Deceased 4th October, 2011.

0005-2728/$ – see front matter © 2011 Elsevier B.V. All rights reserved.
doi:10.1016/j.bbabio.2011.11.005

2. Materials and methods

2.1. Sample preparation

Cytochrome *c* oxidase from *Paracoccus denitrificans* was isolated and prepared as described earlier [13,14]. Reconstitution of the enzyme into vesicles was achieved with Bio-Beads (Bio-Rad Laboratories) using a method described before [15], except that the enzyme concentration during the reconstitution was 6.7 μM. In addition to the wild type enzyme, two batches of mutant enzymes were used, D124N and K354M, the classical D- and K-channel variants, respectively.

2.2. The electrometric setup

The setup was described in detail previously, for example in Refs. [15,16]. In the measuring system a membrane, i.e. a phospholipid impregnated Teflon mesh, divides the measuring cell into two compartments and voltage over the membrane is measured with two Ag/AgCl electrodes (World Precision Instruments), one in each compartment. The vesicles with reconstituted CcO were fused with the measuring membrane by adding 25 mM $MgCl_2$ in 100 mM HEPES (pH 7.5). After incubation for 2 h, the buffer was replaced with the experimental one with the desired pH. Buffers were used at 100 mM final concentration as follows (corresponding pH in parenthesis): MES (6), MOPS (7), HEPES (7.5), TRIS (8 and 8.5), CHES (9 and 9.5), CAPS (10 and 10.5) (all buffers from Sigma). Measurements were conducted under a 100% CO atmosphere and CO photolysis was induced by a laser flash (Brilliant YAG, Quantel, pulse energy = 180 mJ, λ = 532 nm). When multiple averages were taken, laser flashes were separated by a 4–5 s pause. The voltage reported by the system is proportional to charge movement inside the enzyme perpendicular to the membrane plane.

2.3. The measurement procedure

First, the sample was fully reduced by glucose oxidase (0.13–0.27 U/μL, Biozyme Laboratories) and glucose (63 mM, Merck) in the presence of catalase (0.45 U/μL, Sigma), using hexaammineruthenium (1 μM, Aldrich) as a redox mediator. Reduction was followed as the extent of electric potential generation upon electron backflow [17], and the sample was judged to be fully reduced when all traces of backflow (maximal at the 3-electron reduction level of the enzyme [17]) had disappeared. Second, the potential generation by the enzyme was followed after addition of 100 μL of oxygen saturated buffer directly toward the measuring membrane, followed by an immediate laser flash, as described previously [17]. Third, sodium dithionite (Merck) was added to a final concentration of 1.5 mM to both sides of the measuring membrane to reduce the sample and to quickly remove excess oxygen. Time-resolved CO photolysis of fully reduced CcO was then followed after different times of incubation. The transmembrane leak of potential through the measuring membrane was recorded on a second time scale and fitted. These results were then used to compensate the leak especially for the D124N mutant that has a rather slow oxidation rate.

2.4. Data analysis

Custom made Matlab (MathWorks) scripts and functions were used for data treatment, fitting and presentation.

3. Results

3.1. CO photolysis of the fully reduced enzyme

Fig. 1 shows the development of electric potential upon photodissociation of carbon monoxide from CcO that was immediately reduced by dithionite after oxidation by O_2 at pH 9.5. Each trace represents an average of ten flashes fired with 4-second intervals at different times after re-reduction. Upon the laser flash there is a fast 1.5 μs phase, which stays unchanged over the time of the experiment. It is followed by a slow phase (180 μs at this particular pH), the amplitude of which decreases with the time between enzyme re-reduction and CO photolysis. The last phase reflects decay of the potential due to CO recombination, the rate of which becomes faster with time after enzyme activation. Note that CO recombination in the figure is presented on a much slower time scale relative to the two preceding phases (Fig. 1). The dependence of the amplitudes of the first and second phases on the delay between reduction and CO photolysis, obtained as a result of the data fitting process, is presented in Fig. 2. The data shows that the first phase maintains its amplitude over the measuring period, while the second phase fades out completely with a time constant of ~25 min.

3.1.1. The fast phase

The 1.5 μs phase has a constant amplitude and rate from pH 7 to 10 (Supplementary material Fig. S1). Its amplitude starts to drop only at pH 10.5, but at such a high pH part of the enzyme population could already be denatured, or the hemes destroyed [18]. Between pH 7 and 10 the amplitude is 0.83 mV on the average with a standard deviation of 0.13 mV. The average time constant is 1.5 μs (rate $650 \pm 196\ ms^{-1}$). To verify the nature of the potential generation upon CO photolysis

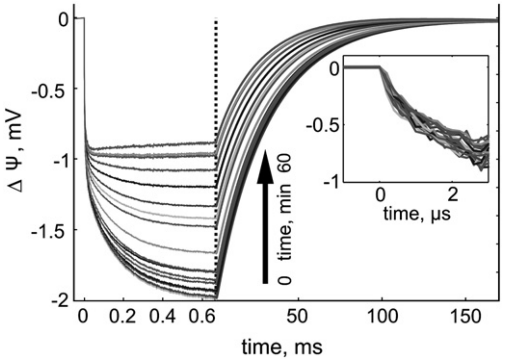

Fig. 1. Electric potential development upon CO photolysis of the fully reduced *Paracoccus denitrificans* aa_3 oxidase at pH 9.5. Reaction starts with the laser flash at time 0. Each curve represents individual time points (time scale minutes), where the first trace is immediately after dithionite re-reduction following activation of the enzyme by turnover. Inset: early part of reaction, up to 3 μs. Conditions: 100 mM CHES, pH 9.5, 1 μM hexamine–ruthenium, 0.45 U/μL catalase, 0.25 U/μL glucose oxidase, 63 mM glucose, 1.5 mM sodium dithionite after 100 μL pulse of O_2 saturated buffer, under 100% CO atmosphere.

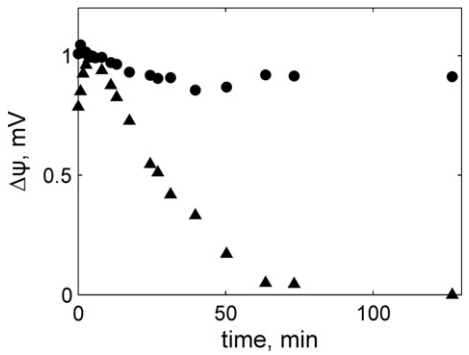

Fig. 2. Dependence of the amplitudes of the fast ~1.1 μs (●) and slow ~180 μs (▲) phases of potential generation upon CO photolysis from the fully reduced CcO on the time after enzyme activation at pH 9.5. Conditions as in Fig. 1.

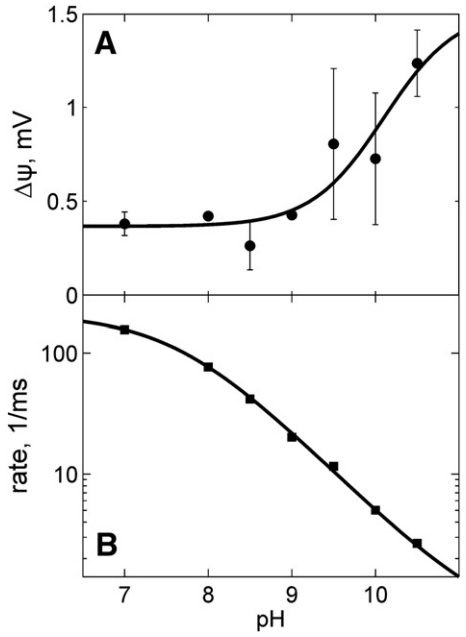

Fig. 3. pH dependence of the slow phase amplitude (A) and rate constant (B) of potential generation upon CO photolysis by the wild type C*c*O. Panel A presents averages of maximum amplitudes (mV) of the second phase. Solid line: Henderson–Hasselbalch fit with pK_a 10.1. Panel B shows averages of corresponding rate constants of the slow phase on a logarithmic scale. Solid line: Henderson–Hasselbalch fit with pK_a 7.7 and Hill coefficient 0.71. Conditions: for every pH value 100 mM buffer (for details see Materials and methods), 1 μM hexamine–ruthenium, 1.5 mM sodium dithionite after 100 μL pulse of O_2 saturated buffer, 0.45 U/μL catalase, 0.13–0.27 U/μL glucose oxidase and 63 mM glucose, under 100% CO atmosphere.

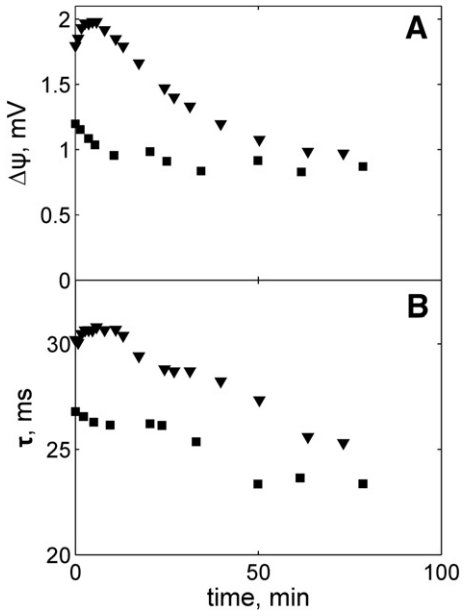

Fig. 4. Dependence of the amplitude (A) and rate constant (B) of potential dissipation upon CO recombination in the wild type C*c*O on the time of the experiments at two pH values—7(■) and 9.5 (▼). Time point 0 is immediately after dithionite re-reduction following oxygen activation of the enzyme. Conditions: as in Fig. 3 (Materials and methods).

we also performed measurements on mutant enzymes which have blocks in either of the two proton-conducting channels. The amplitudes of the first phase for the two studied mutants, D124N and K354M, have exactly the same time constant as wild type enzyme. The amplitude of the first (1.5 μs) phase also does not depend on pH in the D124N variant (Supplementary material Fig. S2). There is a slight decrease in the amplitude of the K354M variant towards the alkaline end of the titration, but this could be due to easier alkaline denaturation of this variant.

3.1.2. The slow phase

In wild type oxidase the slow phase grows to its maximum amplitude in 1 to 3 min after dithionite addition (Fig. 2), and then decreases with a time constant of about 25 min. Fig. 3 presents the amplitudes and rate constants of the second phase as a function of pH in wild type C*c*O. The amplitude increases with pH, becoming larger than the fast phase at the alkaline end of the titration. Conversely, the rate is fast at neutral pH and slows down with pH almost linearly on a logarithmic scale, dropping from an average of 155 ms^{-1} at pH 7 to 2.7 ms^{-1} at pH 10.5. It should be noted that discriminating between the fast and slow phase becomes more difficult as the slow phase speeds up at neutral pH. The slow phase is present in the D124N variant, but it is entirely absent in the K354M variant. The results for the slow phase in mutant enzymes are presented in the supplementary Fig. S3. We also conducted control experiments where we followed CO photolysis for C*c*O that had not been activated by reduction and reoxidation by oxygen. In these controls the amplitude of the slow phase was only 10–30 per cent of that in the pre-activated case.

3.1.3. The decay of electric potential

Upon CO recombination the decay of potential is slower when the amplitude of the signal is larger. In other words, when the slow phase is present, CO recombination is slow and gets faster when the slow phase disappears. This is presented in Fig. 4, where the amplitudes (Fig. 4A) and the time constants (Fig. 4B) of the CO recombination phase of wild type enzyme are compared at pH 7 (■) and 9.5 (▼) at different time points after enzyme activation. The CO recombination rate is quite different for the activated enzyme at these two pH values, but after enzyme relaxation (and disappearance of the slow phase) it became similar (τ ~ 25 ms) to the earlier reported values for the fully reduced enzyme [19,20].

3.2. Oxygen reaction

In the same samples where electric potential generation upon CO photolysis was followed, we also recorded the development of electric potential during the oxidative half of the catalytic cycle triggered by CO photolysis in the presence of O_2. In fact, this measurement was used as the enzyme activation procedure before sample re-reduction with dithionite. The data on electrogenic reactions of fully reduced C*c*O with oxygen, i.e. transition from state **R** (four electron reduced) to state $\mathbf{O_H}$ (oxidized), was obtained as in an earlier study [17]. Here we aimed at comparing amplitudes of this response with the amplitude of the fast 1.5 μs phase, which does not depend on pH, time of the experiment or the mutation type, but rather reflects the amount of CO-photolysable enzyme fused to the measuring membrane. Fig. 5 presents data on the potential generation in **R** to $\mathbf{O_H}$ transitions at different pH values, normalized to the amplitude of the first (1.5 μs) phase of CO photolysis from fully reduced enzyme, for the wild type enzyme (●), and two mutants, K354M (▲) and D124N (■). A Henderson–Hasselbalch one-proton titration curve with pK_a 9.11 is drawn through the wild type data points (for comparison see Ref. [14]). R^2 of the fit was 0.98. As can be noticed, the amplitudes of the oxygen response of the K354M mutant enzyme fit nicely with the wild type data after normalization of the amplitudes to the amplitude of the 1.5 μs phase. Yet, when the measured absolute amplitudes of the oxygen response are compared, the K354M values are smaller and drop faster in alkaline conditions than those of wild type. However, as can be seen from Fig. S2, the amplitude of the 1.5 μs phase in K354M also has a slight tendency to decrease at alkaline pH, and after normalization the ratio of voltage generated by oxygen reaction

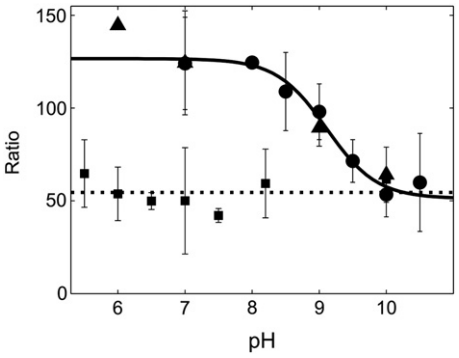

Fig. 5. pH dependence of ratio of the oxygen reaction to the fast phase of CO photolysis. The ratio is calculated by dividing the amplitude of the electric potential generation during the reaction of fully reduced C*c*O with oxygen by the amplitude of the fast phase of CO photolysis reaction measured on the same sample. Data represents wild type (●), K354M mutant (▲) and D124N (■). Henderson–Hasselbalch fit of wild type data (solid line) has pK_a 9.11. Conditions: for every pH 100 mM buffer (for details see Materials and methods), 1 μM hexamine–ruthenium, 0.45 U/μL catalase, 0.13–0.27 U/μL glucose oxidase and 63 mM glucose, under 100% CO atmosphere. In case of K354M 10 μM hexamine–ruthenium was used instead of 1 μM.

to the amplitude of the 1.5 μs phase is the same as in the wild type enzyme. In contrast, the D124N mutant behaves differently. At neutral pH the normalized response is only approximately one half of that in the wild type and the K354M variant, and virtually independent of pH so that the amplitude matches that of the wild type enzyme at high pH. Such behaviour is expected because the D-channel mutant does not pump protons, and only catalyses charge translocation through vectorial chemistry (see Introduction) [21–23].

3.3. Redox state dependence of the fast phase

We have so far reported on the existence of the fast 1.5 μs phase in the fully reduced enzyme. To find out whether this phase depends on the redox state, we performed analogous experiments at different redox potentials. Fig. 6 shows traces upon CO photolysis for non-activated enzyme at pH 8.6. The fast 1.5 μs phase is clearly absent from the mixed valence enzyme ($E_h = 420$ mV), but shows slower charge separation with opposite polarity due to the well-known

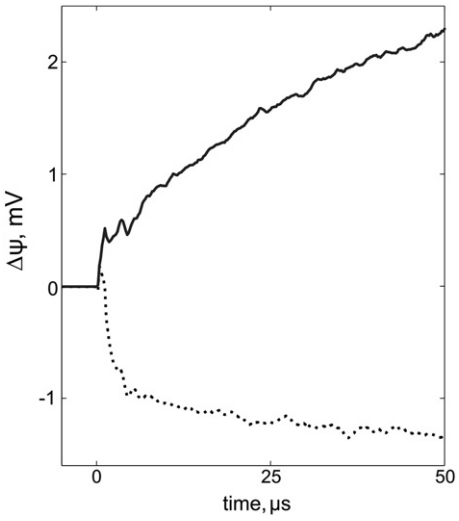

Fig. 6. Potential generation upon CO photolysis in mixed-valence (solid line) and fully reduced (dotted line) *Paracoccus denitrificans* aa_3 oxidase at pH 8.6. Reaction starts with a laser flash at time 0. Conditions: 100 mM bicine (pH 8.6), 0.5 U/μL catalase, 0.2 U/μL glucose oxidase, 63 mM glucose, 1 μM hexamine–ruthenium, under 100% CO atmosphere. Mixed-valence state was induced by adding 15 mM ferri/ferrocyanide with 1:1 stoichiometry. In reduced case $E_h < 190$ mV and in mixed-valence case $E_h = 420$ mV.

proton transfer via the K-pathway coupled to backflow of electrons from the binuclear site at high pH [19,24,25].

3.4. Spectrum of the fast phase

Optical absorption measurements were done to determine the nature of the potential generation phases upon CO photolysis. Experiments were conducted at pH 9.5 where both phases were clearly observable by electrometry. However, freshly oxidized enzyme, re-reduced by dithionite, did not show any significant changes of optical absorbance with a time constant of 180 μs corresponding to the slow phase of potential generation, but clearly showed changes with a time constant of 1.5 μs (Fig. 7). These optical changes are identical to those described earlier at neutral pH [26,27]. Fig. 7A shows a kinetic trace at 613 nm, where this fast change is clearly seen as a decrease of absorbance immediately after the initial increase caused by the scission of the carbon monoxide-heme a_3 bond by the laser flash. Fig. 7B shows the kinetic spectrum of this phase, which has a maximum at 600 nm, a trough at 613 and intersects zero close to 605 nm.

4. Discussion

4.1. Nature of the fast phase

Photolysis of CO from the reduced heme-copper oxidase is quite different from the equivalent process in other heme-containing proteins. The main difference is due to the location of the copper atom (Cu_B) in very close proximity to the iron of heme a_3. Such architecture of the binuclear site results in very fast<1 ps [26,28] initial migration of CO from Fe^{2+}_{a3} to Cu^{+}_{B} upon the laser flash. In the next step, CO dissociates from the Cu_B site with a time constant of about 1.5 μs [29], which coincides well with the time constant of the fast phase of potential generation obtained in our experiments. Thus, it would be natural to propose that the fast phase is the result of CO dissociation from Cu_B. However, as we showed by the redox state dependence (Fig. 6), the reduced and CO-ligated binuclear site is a necessary but insufficient condition for appearance of the fast phase. In the mixed valence enzyme, where the binuclear site has the same electronic state as in the fully reduced enzyme, but where the donor centers (Cu_A and heme *a*) are oxidized, there was no potential generation corresponding to the 1.5 μs phase.

The absorbance changes in the visible region also show a component with a time constant of 1.5 μs. The optical spectrum of this phase has a derivative shape that is characteristic of a blue absorbance band shift with a cross-over point at 605 nm, and maximum and minimum at 600 and 613 nm, respectively. Such properties would be expected for a blue shift of the α-band of low spin ferrous heme *a*. However, Einarsdottir et al. [26], who showed the same

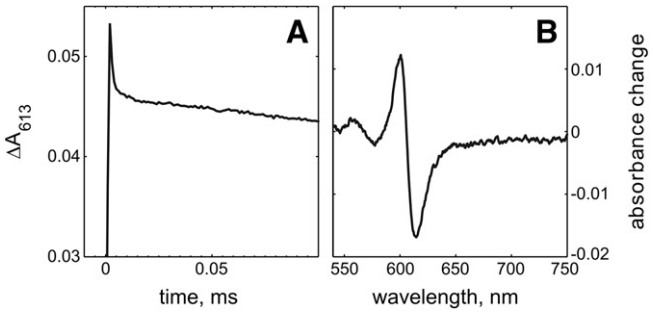

Fig. 7. Absorbance changes upon CO photolysis from fully reduced CO-ligated wild type C*c*O. The time course at 613 nm is shown in panel A. The kinetic spectrum of the 1.5 μs phase as a result of a global fit of the recorded multiwavelength data surface is presented in panel B. Conditions: 200 mM CHES, pH 9.5, 0.05% DM, 10 U/ml glucose oxidase, 10 mM glucose, 30 U/ml catalase, 1 μM hexamine–ruthenium ($[Ru(NH_3)_6]^{2+/3+}$), under 100% CO atmosphere.

blue shift with similar kinetics in enzyme from bovine heart mitochondria, found it to occur not only in fully reduced enzyme, but also in the mixed-valence state with only slightly smaller amplitude. It is clear, therefore, that the 1.5 μs optical shift differs from the 1.5 μs charge separation in that the latter is not observed in the mixed-valence enzyme.

On the basis of the information at hand, it seems that the 1.5 μs charge separation phase is kinetically limited by the rate of CO dissociation from Cu_B. However, the absence of this phase in the mixed-valence enzyme is enigmatic because CO dissociation, as such, is not affected by the redox states of heme *a* or Cu_A. The insensitivity of this phase to variations in pH and to key mutations in proton transfer pathways provides no support for net proton transfer as the cause, and electron transfer is excluded in the fully reduced enzyme. The 1.5 μs phase seems to be a fully conserved feature among diverse members of the vast heme-copper oxidase family (ba_3 and caa_3 from *Thermus thermophilus*, cbb_3 from *Rhodobacter sphaeroides*, data not shown). We may speculate that dissociation of CO from Cu_B induces a rearrangement of ligands to both Cu_B and heme a_3. These could be water molecules, whose arrangement may depend on the redox state of heme *a* [30]. Rearrangement due to CO dissociation from Cu_B could change the overall dipole moment of a cluster of water molecules to mimic a 0.83 Å movement of an elementary charge perpendicular to the membrane plane.

4.2. Amplitude of the fast phase

In our experiments we were able to sequentially measure the potential generation from the same sample for two cases: CO photolysis, and the reaction of C*c*O with oxygen under the same experimental conditions. For the fully reduced enzyme the ratio of amplitudes of the oxygen response to the fast phase of CO photolysis (125, see Fig. 5) is very stable, even though the absolute values of the amplitudes vary depending on conditions of the experiment and sample preparation. From this ratio we can estimate the dielectric distance of charge separation due to CO photolysis. For that purpose we have to know the number of charges translocated during the reaction of fully reduced enzyme with oxygen. This number can be estimated based on the current knowledge of the enzyme structure and its location in the membrane dielectric [31]. Our earlier measurements [22] showed that during the oxidative phase two pumped protons are translocated across the whole membrane. In addition, the redox chemistry results in vectorial electrogenic events: two “chemical” protons are taken up to the binuclear center from the N side, and are translocated through about 2/3 of the membrane dielectric where they meet an electron delivered via 1/3 of the membrane dielectric from Cu_A at the P side of the membrane. Altogether, these events make the net number of translocated charges $2+2\times2/3+1/3=3.7$. The measured potential is thus the result of translocation of 3.7 charges across 28 Å of the hydrophobic membrane core [32]. The response of CO photolysis is 125 times smaller, which would be equivalent to translocation of one charge across $3.7\times28/125=0.83$ Å in a direction perpendicular to the membrane. This tiny charge movement can be recorded very well by our method and, most importantly, it can be used as an internal ruler for the calibration of charge translocation events in the enzyme. Additionally, it is important to note that the fast phase of CO photolysis was present in both mutant enzymes tested, as well as in other types of oxidases (see above). As an illustration of the applicability for this "dielectric ruler" we analyzed two well-characterized mutants of C*c*O. It was earlier shown [21–23] that the K354M mutation, which blocks the K channel, does not influence proton translocation during the oxidative phase of enzyme turnover. The measurements presented in this work confirmed this finding: the ratio of the amplitude of the electrometric oxygen response to the fast phase of CO photolysis in the K354M mutant is the same as in the wild type enzyme (i.e. 125, see Fig. 5). It should be stressed that the absolute amplitude of the oxygen response at neutral pH for the K354M mutant is only around 50 mV, which is about twice smaller than that for the wild type enzyme. Thus, the use of absolute values of potential generation for comparison of the K354M mutant with wild type is not possible. At the same time, the mutation in the D-channel (D124N) decreases this ratio to 54.5, which is equivalent to translocation of a single charge across a $54.5\times0.83=45.2$ Å barrier. Or, taking into account the thickness of the membrane dielectric (28 Å), we find the number of charges translocated by the D124N mutant during the oxidative phase of the catalytic cycle to be $45.2/28=1.62$. This number is smaller by ~2 charges than the one for the wild type enzyme (3.7, see above), and correlates well with the knowledge [33] that 2 protons are pumped during the oxidative phase of the catalytic cycle in the wild type enzyme, and that proton pumping is abolished in the D124N mutant.

4.3. pH dependence of the charge separation in the oxidative half of the catalytic cycle

A comparison of the potential changes at neutral and alkaline pH values was done earlier [2,14,34]. Previous results were based on the total potential change associated with oxidation of C*c*O, and did not take into account the decline of the amount of active enzyme at alkaline pH. Here, in Fig. 5, we presented the response [14,34,35] normalized to the fraction of the enzyme active in CO photolysis. We recognize that there are problems in the assumption that all the signals decrease in exactly the same manner as the enzyme denatures. Despite that, the normalization of the oxygen responses with CO photolysis from fully reduced C*c*O ties mutants with different response amplitudes nicely together, which is especially noticeable in the case with wild type and K354M mutant (see above). In a previous study [14] the amplitudes of potential generation upon addition of oxygen at alkaline pH tended to approach zero. However, normalization with the amplitude of the CO photolysis effect changes the picture. The normalization shows that at alkaline pH the potential approaches 40% of the signal obtained at neutral pH, which corresponds to translocation of $3.7\times0.4=1.48$ charges. Loss of about 2 translocated charges at high pH is consistent with disappearance of proton pumping at alkaline pH [35]. The fit of the data by the Henderson–Hasselbalch equation (solid curve, Fig. 5) shows that proton pumping disappears in the aa_3 oxidase from *P. denitrificans* with an apparent pK_a of ~9.1. The fact that the pH dependence is absent in the non-pumping D124N mutant enzyme, where the amplitude is close to that in wild type at very high pH, provides further support for our conclusion.

4.4. The nature and origin of the slow phase

The relaxation of the oxidized enzyme to the non-active “resting” form of the “fast” [36], “pulsed” [37] or active [33] forms of C*c*O is well documented in the literature. Here we showed that the protein relaxation kinetics is clearly seen also for the reduced form of the enzyme. This conclusion is based on the time dependence of the amplitude of the slow phase of potential generation upon CO photolysis after enzyme turnover (Fig. 2), which diminishes with a time constant of ~25 min after a single turnover of C*c*O (oxygen injection and CO photolysis was followed by immediate enzyme reduction). As may be noted from Fig. 2, in the first moments after the addition of dithionite the amplitude of the slow phase seems to be growing with a time constant of about 1 min. The source of this effect is not completely clear, but it may be induced by a small oxygen contamination of the system from, for example, the needle by which dithionite was injected. Such a contamination could result in the electron backflow reaction and accompanying proton transfer [19]. At pH 9.5 the backflow reaction would result in potential generation of the opposite sign from the slow phase, thus decreasing the slow phase signal. If

this explanation is true, we estimate the amount of oxygen-contaminated protein to be about 4%.

What could be the possible cause of the slow phase of potential generation upon CO photolysis? Transmembrane electron transfer can be excluded since the enzyme is fully reduced. The strong pH dependence argues in favour of movement of a proton within the protein core, perpendicular to the membrane plane. The amplitude increases dramatically at alkaline pH, which means that the acceptor group involved should have an alkaline pK_a in order to be unprotonated before excitation, and to be able to take the proton after the laser flash. For practical reasons we could not go to pH values higher than 10.5 to finish the titration. However, it is clear that the amplitude is still increasing at the alkaline edge and even though we could not exactly define the pK_a of this transition, its low limit can be estimated as ~10.1 (Fig. 3), but the true value is likely to be higher (see below). The abolition of this phase in the K354M variant provides an important clue to its nature. Lysine 354 itself could be the group responsible, in which case the phase is due to electrogenic proton uptake from the N phase to the lysine. The pH dependence of the amplitude of the slow phase found in our investigation is indeed rather similar to the pH dependence of the K354 protonation state for the fully reduced enzyme obtained from electrostatic calculations [38].

The pH dependence of the rate of the slow phase (Fig. 3B) shows that this rate is controlled by the degree of protonation of another group with a pK_a of ~7.7. In accordance with the scenario suggested above, K354 would be in protonic equilibrium with the N phase via the input amino acid of the K-pathway, E(II)-78 (Fig. 8). The observed pK_a of 7.7 for the group controlling the rate is indeed close to the pK_a value for E(II)-78 found in continuum electrostatic calculations of the fully reduced CcO [38]. It also correlates well with the value found for the pH dependence of the alkaline-induced electron backflow [24], which is now established [19,25] to be coupled to proton release through the K channel from a water molecule bound to the ferric a_3 heme.

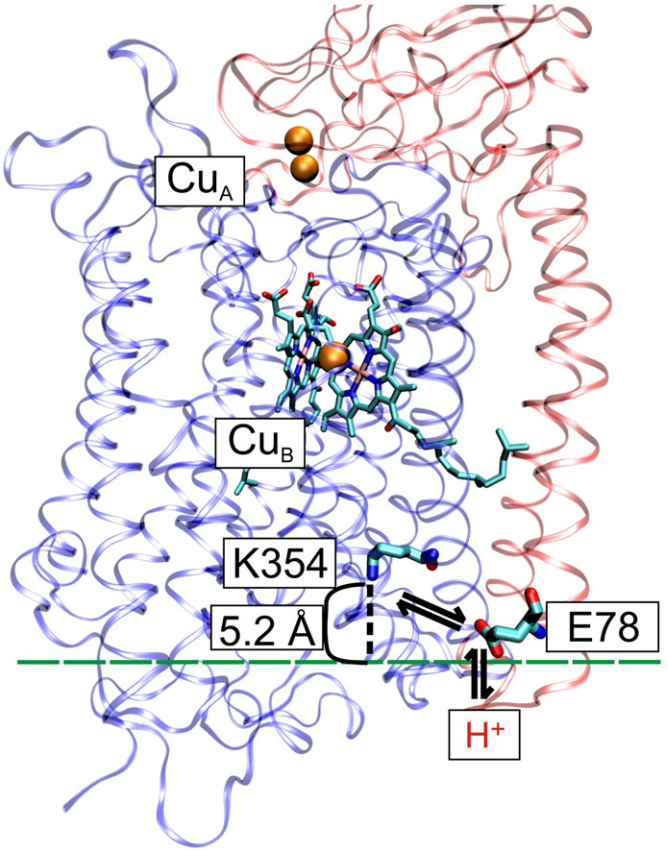

Fig. 8. Structure of CcO subunits I and II based on PDB ID: 3HB3 [42]. Cu_A and Cu_B, hemes *a* and a_3 are highlighted together with K-pathway residues K354 and E78. The figure was prepared using VMD software [43].

The following analysis supports the notion that the amplitude of the second phase is linked to the protonation state of lysine 354. The dielectric topography map [9] gives the value of the relative dielectric depth of this residue as 0.186 when counted from the N side of the membrane from where the proton is taken up according to our model (Fig. 8). When taking into account the thickness of the membrane dielectric and the dielectric ruler obtained in this work (0.83 mV/Å), the expected maximal amplitude of potential generation should be 28 Å × 0.186 × 0.83 mV/Å = 4.3 mV when the lysine is initially unprotonated and takes up one full proton. In our experiments the largest amplitude was ~1.3 mV observed at pH 10.5 (Fig. 3), which is 30% of the estimated maximum, and higher pH values were not attempted due to enzyme denaturation. Continuum electrostatic calculations with fully reduced enzyme [38] predict that K354 is ~75% protonated at pH 10.5, so that maximally 25% can be further protonated, which is in remarkable agreement with the experimental results.

The emerging picture is thus that the slow electrometric phase following CO photolysis from fully reduced enzyme is due to (fractional) proton uptake via the K-pathway into K354, from the N side of the membrane. The most plausible reason for this is evidently an increase in the pK_a of K354 caused by the dissociation of CO from the binuclear site. However, considering that the distance from K354 to the binuclear site is nearly 20 Å, such an effect is by no means obvious. Perturbance of the structure of water molecules within the K-pathway is expected to change the pK_a of K354 [38,39]. Moreover, Qin et al. [40] have shown crystallographic evidence for redox-and ligand-dependent changes in the water structure at the end of the K-pathway, close to the binuclear site. It seems feasible, therefore, that dissociation of CO from the active site changes the water structure along the K-pathway in such a way as to cause an increase in the pK_a of the lysine.

Another possible reason for the slow electrometric phase is a "flip" of the protonated side chain of K354 "upwards" from the position in the crystal structure (Fig. 8). However, it may be less evident why such a reorientation would show the observed pH dependence. At any rate, such a side chain reorganisation could occur in conjunction with proton uptake, although the above analysis does not require it.

4.5. The effect of enzyme activation

The molecular basis for the fact that proton translocation in the reductive phase of the catalytic cycle requires "activation" of the enzyme by prior reduction and reoxidation by O_2 [22,33] is not understood. Here, we showed that such "activation" also affects the state of the fully reduced enzyme, in that the slow electrometric phase was much diminished in amplitude if the enzyme was not pre-activated, and that it disappeared completely after a sufficiently long incubation in the reduced state prior to the laser pulse (Fig. 2). In view of the discussion above, it would seem plausible that "activation" involves the reorganisation of water molecules in the K-pathway, or filling strategic positions in that pathway with water (see Ref. [41]). In fact, none of the available crystal structures show a continuous water array in the K-pathway, in contrast to the very well developed water file in the lower parts of the D-pathway (see e.g. Ref. [40]).

Supplementary materials related to this article can be found online at doi:10.1016/j.bbabio.2011.11.005.

Acknowledgements

This work was supported by Biocentrum Helsinki, the Sigrid Jusélius Foundation and the Academy of Finland. We are grateful to Prof. Mårten Wikström for the critical comments and invaluable help in the writing and preparation of the manuscript.

References

[1] P. Mitchell, Coupling of phosphorylation to electron and hydrogen transfer by a chemi-osmotic type of mechanism, Nature 191 (1961) 144–148.
[2] M.K. Wikström, Proton pump coupled to cytochrome *c* oxidase in mitochondria, Nature 266 (1977) 271–273.
[3] P.E. Siegbahn, M.R. Blomberg, Proton pumping mechanism in cytochrome c oxidase, J. Phys. Chem. A 112 (2008) 12772–12780.
[4] M. Wikström, M.I. Verkhovsky, Mechanism and energetics of proton translocation by the respiratory heme-copper oxidases, Biochim. Biophys. Acta 1767 (2007) 1200–1214.
[5] I. Belevich, M.I. Verkhovsky, Molecular mechanism of proton translocation by cytochrome *c* oxidase, Antioxid. Redox Signal. 10 (2008) 1–29.
[6] G. Brändén, R.B. Gennis, P. Brzezinski, Transmembrane proton translocation by cytochrome *c* oxidase, Biochim. Biophys. Acta 1757 (2006) 1052–1063.
[7] L.A. Drachev, A.D. Kaulen, V.P. Skulachev, Time resolution of the intermediate steps in the bacteriorhodopsin-linked electrogenesis, FEBS Lett. 87 (1978) 161–167.
[8] M.I. Verkhovsky, J.E. Morgan, M.L. Verkhovskaya, M. Wikström, Translocation of electrical charge during a single turnover of cytochrome *c* oxidase, Biochim. Biophys. Acta 1318 (1997) 6–10.
[9] R. Sugitani, E.S. Medvedev, A.A. Stuchebrukhov, Theoretical and computational analysis of the membrane potential generated by cytochrome *c* oxidase upon single electron injection into the enzyme, Biochim. Biophys. Acta 1777 (2008) 1129–1139.
[10] J. Deisenhofer, O. Epp, K. Miki, R. Huber, H. Michel, X-ray structure analysis of a membrane protein complex. Electron density map at 3 Å resolution and a model of the chromophores of the photosynthetic reaction center from *Rhodopseudomonas viridis*, J. Mol. Biol. 180 (1984) 385–398.
[11] S.K. Chamorovsky, D.A. Cherepanov, C.S. Chamorovsky, A.Y. Semenov, Correlation of electron transfer rate in photosynthetic reaction centers with intraprotein dielectric properties, Biochim. Biophys. Acta 1767 (2007) 441–448.
[12] A. Semenov, D. Cherepanov, M. Mamedov, Electrogenic reactions and dielectric properties of photosystem II, Photosynth. Res. 98 (2008) 121–130.
[13] S. Riistama, L. Laakkonen, M. Wikström, M.I. Verkhovsky, A. Puustinen, The calcium binding site in cytochrome aa_3 from *Paracoccus denitrificans*, Biochemistry 38 (1999) 10670–10677.
[14] C. Ribacka, M.I. Verkhovsky, I. Belevich, D.A. Bloch, A. Puustinen, M. Wikström, An elementary reaction step of the proton pump is revealed by mutation of tryptophan-164 to phenylalanine in cytochrome *c* oxidase from *Paracoccus denitrificans*, Biochemistry 44 (2005) 16502–16512.
[15] M.I. Verkhovsky, A. Tuukkanen, C. Backgren, A. Puustinen, M. Wikström, Charge translocation coupled to electron injection into oxidized cytochrome *c* oxidase from *Paracoccus denitrificans*, Biochemistry 40 (2001) 7077–7083.
[16] D.A. Bloch, A. Jasaitis, M.I. Verkhovsky, Elevated proton leak of the intermediate O_H in cytochrome *c* oxidase, Biophys. J. 96 (2009) 4733–4742.
[17] A. Jasaitis, M.I. Verkhovsky, J.E. Morgan, M.L. Verkhovskaya, M. Wikström, Assignment and charge translocation stoichiometries of the major electrogenic phases in the reaction of cytochrome *c* oxidase with dioxygen, Biochemistry 38 (1999) 2697–2706.
[18] P.M. Callahan, G.T. Babcock, Origin of the cytochrome *a* absorption red shift: a pH-dependent interaction between its heme a formyl and protein in cytochrome oxidase, Biochemistry 22 (1983) 452–461.
[19] I. Belevich, A. Tuukkanen, M. Wikström, M.I. Verkhovsky, Proton-coupled electron equilibrium in soluble and membrane-bound cytochrome *c* oxidase from *Paracoccus denitrificans*, Biochemistry 45 (2006) 4000–4006.
[20] I. Szundi, J. Ray, A. Pawate, R.B. Gennis, Ó. Einarsdóttir, Flash-photolysis of fully reduced and mixed-valence CO-bound *Rhodobacter sphaeroides* cytochrome *c* oxidase: heme spectral shifts, Biochemistry 46 (2007) 12568–12578.
[21] P. Ädelroth, R.B. Gennis, P. Brzezinski, Role of the pathway through K(I-362) in proton transfer in cytochrome *c* oxidase from *R. sphaeroides*, Biochemistry 37 (1998) 2470–2476.
[22] D. Bloch, I. Belevich, A. Jasaitis, C. Ribacka, A. Puustinen, M.I. Verkhovsky, M. Wikström, The catalytic cycle of cytochrome *c* oxidase is not the sum of its two halves, Proc. Natl. Acad. Sci. U. S. A. 101 (2004) 529–533.
[23] A.A. Konstantinov, S. Siletsky, D. Mitchell, A. Kaulen, R.B. Gennis, The roles of the two proton input channels in cytochrome *c* oxidase from *Rhodobacter sphaeroides* probed by the effects of site-directed mutations on time-resolved electrogenic intraprotein proton transfer, Proc. Natl. Acad. Sci. U. S. A. 94 (1997) 9085–9090.
[24] S. Hallen, P. Brzezinski, B.G. Malmström, Internal electron transfer in cytochrome *c* oxidase is coupled to the protonation of a group close to the bimetallic site, Biochemistry 33 (1994) 1467–1472.
[25] Brändén, A. Namslauer, O. Hansson, R. Aasa, P. Brzezinski, Water-hydroxide exchange reactions at the catalytic site of heme-copper oxidases, Biochemistry 42 (2003) 13178–13184.
[26] O. Einarsdottir, R.B. Dyer, D.D. Lemon, P.M. Killough, S.M. Hubig, S.J. Atherton, J.J. Lopez-Garriga, G. Palmer, W.H. Woodruff, Photodissociation and recombination of carbonmonoxy cytochrome oxidase: dynamics from picoseconds to kiloseconds, Biochemistry 32 (1993) 12013–12024.
[27] A. Namslauer, M. Branden, P. Brzezinski, The rate of internal heme–heme electron transfer in cytochrome C oxidase, Biochemistry 41 (2002) 10369–10374.
[28] P.O. Stoutland, J.-C. Lambry, J.-L. Martin, W.H. Woodruff, Femtosecond dynamics of reduced cytochrome oxidase and its CO derivative, J. Phys. Chem. 95 (1991) 6406–6408.
[29] R.B. Dyer, O. Einarsdóttir, P.M. Killough, J.J. López-Garriga, W.H. Woodruff, Transient binding of photodissociated CO to CuB^+ of eukaryotic cytochrome oxidase at ambient temperature. Direct evidence from time-resolved infrared spectroscopy, J. Am. Chem. Soc. 111 (1989) 7657–7659.
[30] M. Wikström, M.I. Verkhovsky, G. Hummer, Water-gated mechanism of proton translocation by cytochrome *c* oxidase, Biochim. Biophys. Acta 1604 (2003) 61–65.
[31] I.V. Leontyev, A.A. Stuchebrukhov, Dielectric relaxation of cytochrome *c* oxidase: comparison of the microscopic and continuum models, J. Chem. Phys. 130 (2009) 085103.
[32] N. Kucerka, S. Tristram-Nagle, J.F. Nagle, Closer look at structure of fully hydrated fluid phase DPPC bilayers, Biophys. J. 90 (2006) L83–L85.
[33] M.I. Verkhovsky, A. Jasaitis, M.L. Verkhovskaya, J.E. Morgan, M. Wikström, Proton translocation by cytochrome *c* oxidase, Nature 400 (1999) 480–483.
[34] H. Lepp, P. Brzezinski, Internal charge transfer in cytochrome c oxidase at a limited proton supply: proton pumping ceases at high pH, Biochim. Biophys. Acta 1790 (2009) 552–557.
[35] M. Verkhovskaya, M. Verkhovsky, M. Wikström, pH dependence of proton translocation by *Escherichia coli*, J. Biol. Chem. 267 (1992) 14559–14562.
[36] A.J. Moody, C.E. Cooper, P.R. Rich, Characterisation of 'fast' and 'slow' forms of bovine heart cytochrome-*c* oxidase, Biochim. Biophys. Acta 1059 (1991) 189–207.
[37] E. Antonini, M. Brunori, A. Colosimo, C. Greenwood, M.T. Wilson, Oxygen "pulsed" cytochrome *c* oxidase: functional properties and catalytic relevance, Proc. Natl. Acad. Sci. U. S. A. 74 (1977) 3128–3132.
[38] A. Tuukkanen, M.I. Verkhovsky, L. Laakkonen, M. Wikstrom, The K-pathway revisited: a computational study on cytochrome c oxidase, Biochim. Biophys. Acta 1757 (2006) 1117–1121.
[39] M. Bränden, H. Sigurdson, A. Namslauer, R.B. Gennis, P. Ädelroth, P. Brzezinski, On the role of the K-proton transfer pathway in cytochrome *c* oxidase, Proc. Natl. Acad. Sci. U. S. A. 98 (2001) 5013–5018.
[40] L. Qin, J. Liu, D.A. Mills, D.A. Proshlyakov, C. Hiser, S. Ferguson-Miller, Redox-dependent conformational changes in cytochrome a oxidase suggest a gating mechanism for proton uptake, Biochemistry 48 (2009) 5121–5130.
[41] V.R.I. Kaila, M.I. Verkhovsky, M. Wikstrom, Proton-coupled electron transfer in cytochrome oxidase, Chem. Rev. 110 (2010) 7062–7081.
[42] J. Koepke, E. Olkhova, H. Angerer, H. Muller, G. Peng, H. Michel, High resolution crystal structure of *Paracoccus denitrificans* cytochrome c oxidase: new insights into the active site and the proton transfer pathways, Biochim. Biophys. Acta 1787 (2009) 635–645.
[43] W. Humphrey, A. Dalke, K. Schulten, VMD: visual molecular dynamics, J. Mol. Graph. 14 (1996) 33–38.